JOURNAL OF MATERIALS SCIENCE 27 (1992) 1926–1932

Joining of silicon nitride to SUS304 stainless steel using a sputtering method

H. SUEYOSHI, M. TABATA, Y. NAKAMURA
Department of Mechanical Engineering II, Kagoshima University, 1-21-40 Korimoto, Kagoshima 890, Japan
R. TANAKA
Department of Mechanical Engineering and Materials Science, Yokohama National University, 156 Tokiwadai, Hodogayaku, Yokohama 240, Japan

Silicon nitride with thin sputter-deposited titanium and nickel films was joined to SUS304 stainless steel (18% Cr–8% Ni) using metallic buffers in a series of silicon nitride/nickel/molybdenum/nickel/SUS304, and the joining strength and microstructures were investigated. Four-point bending tests showed fracture strength of the joints up to 169 MPa. Cracks were formed at the interface between the silicon nitride and its adjacent nickel buffer, and frequently extended into the silicon nitride. Microstructural analyses revealed that the silicon nitride reacted with the sputter-deposited titanium producing titanium nitride and isolated silicon atoms, and that silicon and titanium diffused into the nickel buffer. Calculations using a finite-element method indicated a marked reduction in thermal stress induced in the joined silicon nitride with increasing thickness of the molybdenum buffer. The strong interfacial bond inducing the fracture of the joined silicon nitride was interpreted in terms of a good interfacial reaction, the interdiffusions and the reduction of thermal stress being due to the insertion of the molybdenum buffer.

1. Introduction

Silicon nitride shows high-temperature mechanical properties superior to those of metallic materials. However its brittleness at room temperature is detrimental to structural use. Therefore joining silicon nitride to structural metals may be expected to produce a good structural integrity [1–5]. A commonly utilized and convenient method is to braze ceramics to metals with solders containing active elements such as titanium and zirconium [6]. The usable temperatures of the joints, however, should be kept well below the low melting temperatures of the solders. Thus it is considered that solid-state joining [7, 8] would be a preferable method to produce ceramic/metal joints with a good high-temperature performance, as it may keep firm interfacial bonds even at high temperatures.

Essential elements of strong joints are strong interfacial bonds between ceramics and metals, and reduced thermal stress induced on cooling from joining temperature to room temperature, arising from the different thermal expansion coefficients of ceramics and metals. It is anticipated that the interfacial bond depends strongly on the reaction products at the interface. In particular, it is considered that the insertion of a thin titanium interlayer between metals and ceramics brings about good bonding, as titanium is chemically active to react both with ceramics and metals at high temperature [5]. A silicon nitride/2-mm-thick titanium couple, however, cannot be bonded as titanium silicide is formed in addition to the formation of titanium nitride to induce peeling off at the titanium nitride/titanium silicide interface [5]. This result suggests that the thickness of the titanium interlayer is an important factor.

Several methods have been proposed to reduce the thermal stress and may be classified into two groups. One is the insertion of soft metals such as aluminium and copper between joined metals and ceramics to relax the thermal stress plastically; the other is the insertion of hard metals such as kovar, molybdenum and tungsten possessing thermal expansion coefficients between those of joined metals and ceramics. The combination of these soft and hard metallic buffers may bring about a large reduction in thermal stress.

In the present study, silicon nitride with thin sputter-deposited titanium and nickel films was joined to SUS304 stainless steel (18% Cr–8% Ni; SUS is a symbol for stainless steel in Japanese Industrial Standard) with nickel and molybdenum buffers, and the strength and microstructure of the joints were examined. Elastic analysis of thermal stress induced in the joined specimens was carried out using a finite-element method to estimate the effects of metallic buffers on the reduction of thermal stress induced in the joined silicon nitride.

2. Experimental procedure

2.1. Joining process

Silicon nitride with sintering additives (supplied from Kyocera Co, Kokubu-shi, Kagoshima 899-43, Japan.)

0022–2461 © *1992 Chapman & Hall*

and SUS304 stainless steel were cut and polished mechanically into 17-mm-long specimens with a rectangular cross-section of 3.65×4.55 mm. An RF (Radio Frequency)-sputtering method was used to form titanium films of 0.20, 0.25 and 0.50 μm thickness on surfaces of silicon nitride specimens to be joined. Subsequently the titanium films were covered with 0.50-μm-thick nickel films using the RF-sputtering method in order to avoid oxidation of the titanium films during joining at high temperature. Two nickel sheets of 0.5 mm thickness and a molybdenum sheet of 1 mm thickness were inserted between the silicon nitride and SUS304 stainless steel, as shown in Fig. 1. These nickel buffers were inserted to achieve the joints of nickel film/molybdenum and molybdenum/SUS304. Joining of the specimens was carried out in a vacuum of 1.3×10^{-2} Pa using an RF-induction furnace as shown in Fig. 2 in two steps mentioned below. In the first step, the silicon nitride with the sputter-deposited titanium and nickel films was longitudinally compressed to a pair of nickel and molybdenum buffers with a stress of about 30 MPa. They were heated up to 1423 K in 1.8 ks, kept at this temperature for 1.8 ks, cooled to about 850 K in 1.8 ks and then down to room temperature by cutting off the RF power supply. In the second step, the other nickel buffer and SUS304 stainless steel were set on this joint and then compressed under a stress of 5.6 MPa. They were heated at 1323 K for 900 s with nearly the same heating and cooling rates as those used in the first step.

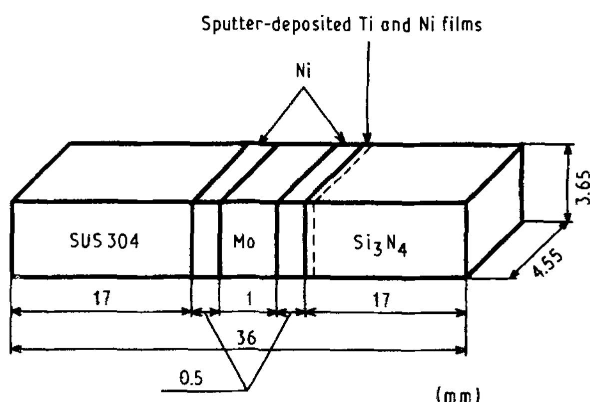

Figure 1 Configuration and size (mm) of specimens.

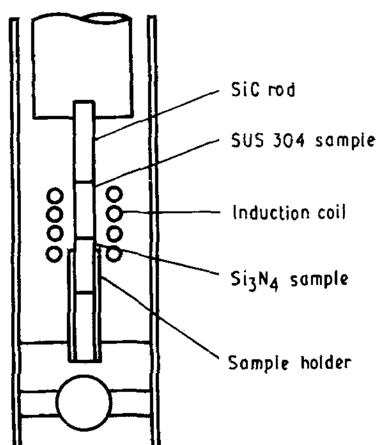

Figure 2 Schematic diagram of joining system using a RF-induction furnace.

The compression stress and heating temperature in the second joining step were reduced to avoid buckling of the SUS304.

2.2. Bending test and microstructural analyses of joints

The fracture stresses of the joints were measured with a four-point bending test at room temperature. Fracture modes were observed using an optical microscope, and microstructural analyses were carried out with an electron probe microanalyser (EPMA).

Films of titanium and nickel deposited on silicon nitride without sintering additives were analysed with an X-ray diffractometer after the heating at 1423 K for 1.8 ks in a vacuum of 1.3×10^{-2} Pa, to examine whether chemical reactions occur between the silicon nitride and deposited films. The chemical forms of elements involved in the films and the substrate were also examined as a function of the depth using electron spectroscopy for chemical analysis (ESCA).

2.3. Thermal stress analysis

Thermal stress induced in the silicon nitride joined to SUS304 on cooling from 1423 K to room temperature was calculated by means of a two-dimensional finite-element method. Elastic moduli, Poisson's ratios and thermal expansion coefficients used in the calculations are listed in Table I. The influence of the inserted nickel and molybdenum buffers on the reduction of the thermal stress was estimated as a function of thickness.

3. Results and discussion

3.1. Fracture strength and modes

Table II shows typical fracture stresses and fracture modes of the joined specimens obtained by the four-point bending test. Initial cracks were formed at the

TABLE I Elastic moduli, Poisson's ratios and thermal expansion coefficients used for finite element calculations

Material	Elastic modulus ($\times 10^5$ MPa)	Poisson's ratio	Thermal expansion coefficient ($\times 10^{-6}$/K)
Si_3N_4	3.00	0.28	3.6
Mo	3.25	0.31	5.6
Ni	1.96	0.30	18.0
SUS304	1.96	0.30	18.7

TABLE II Typical fracture stresses and fracture modes of joints obtained by a four-point bending test

Thickness of sputter-deposited Ti film (μm)	Fracture stress (MPa)	Fracture mode
0.20	146	II
0.25	169	II
0.25	127	II
0.50	78	II
0.50	75	I

interface between the silicon nitride and the adjacent nickel buffer. They propagated along the interface (hereafter called fracture mode I) or extended into the silicon nitride (hereafter called fracture mode II). It is obvious that fracture stresses of mode II are larger than those of mode I, and show values up to 169 MPa. The propagation of cracks from the interface into the silicon nitride suggests the formation of a strongly bonded interface, compared with the silicon nitride. It is considered that the initial crack acts as a deep notch, leading to a much lower apparent bonding strength of the interface than its net bonding strength. In addition, fracture stress is larger in the specimens with 0.20- and 0.25-μm-thick titanium films than in those with 0.50-μm-thick titanium films. This result suggests that the interfacial bonding becomes stronger with a decrease in thickness of the sputter-deposited titanium film.

3.2. EPMA analyses at silicon nitride/nickel buffer interface

Fig. 3 shows typical cross-sectional views traversing the interface between silicon nitride and the adjacent nickel buffer in the specimens which fractured in mode II. Voids were formed at a distance corresponding to the thickness of the sputter-deposited titanium films from silicon nitride in each specimen, distributing themselves parallel to the interface. The density of voids increased with the thickness of the titanium film.

Fig. 4 shows X-ray line profiles of silicon, nickel and titanium across the interface shown in Fig. 3b. Titanium diffused into nickel buffer to a distance of several micrometres. The diffusion distance was identical in all specimens irrespective of the thickness of the titanium film, while the amount of titanium diffusing into the nickel buffer increased with the thickness of the titanium film. Fig. 5 shows X-ray line profiles of silicon and titanium obtained when the sensitivity of the detector for silicon was raised. Silicon diffused into the nickel buffer to a distance of about 20 μm from the interface. The diffusion of titanium and nickel into the joined silicon nitride is not clear from Figs 4 and 5.

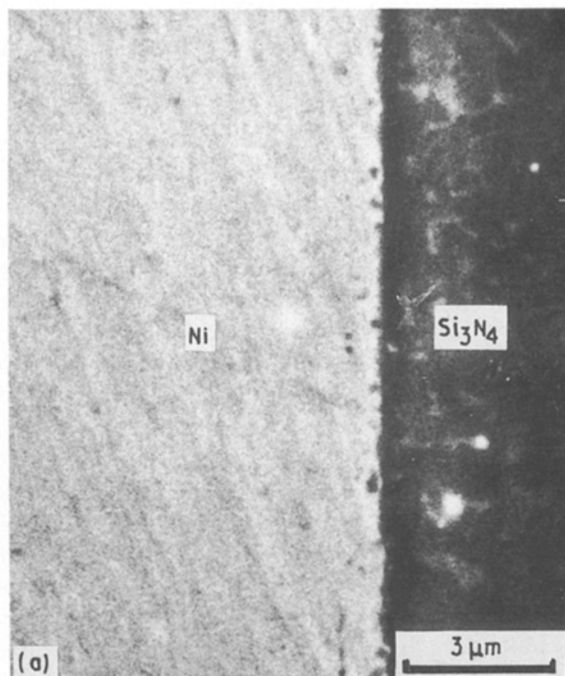

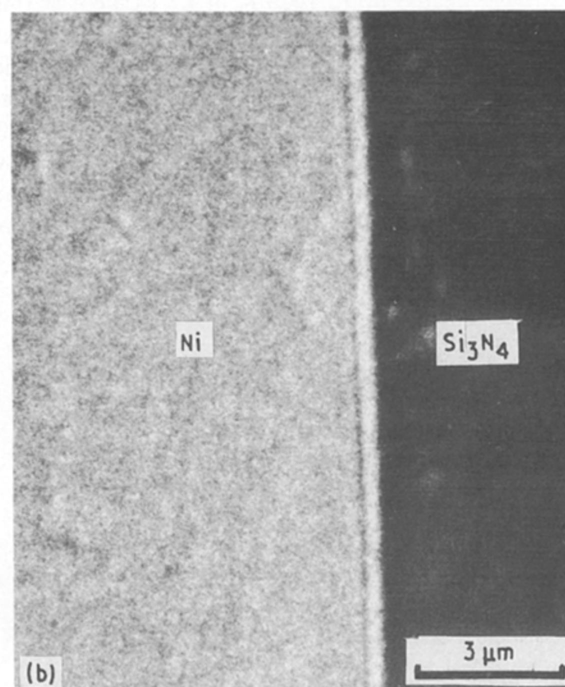

Figure 3 Photographs of secondary electron images of cross-sections traversing the interface between silicon nitride and the adjacent nickel buffer in specimens which fractured in mode II. Thicknesses of sputter-deposited titanium films of the specimens: (a) 0.25; (b) 0.50 μm.

3.3. Interfacial reactions

Fig. 6 shows X-ray diffraction profiles from silicon nitride without sintering additives and from the silicon nitride sputter-deposited with titanium and nickel followed by heating at 1423 K in a vacuum of 1.3 $\times 10^{-2}$ Pa. The profile of silicon nitride without the sputter-deposited films only shows its diffraction peaks (Fig. 6a). The profile of silicon nitride with the sputter-deposited films shows the diffraction peaks of silicon nitride and nickel, but not titanium (Fig. 6b). The diffraction peaks of titanium nitride appear instead of the lack of titanium peaks. The peaks of silicide (Ti_5Si_3), which were formed in the silicon nitride/2-mm-thick titanium couple [5], cannot be recognized in this profile.

ESCA analyses were carried out to reveal the chemical shifts of elements involved in the sputter-deposited films and silicon nitride at the interface. Fig. 7 shows the change in chemical forms of nickel, silicon and nitrogen with depth from the surface of the sputter-deposited nickel film to the silicon nitride. The profile of Fig. 7a shows that nickel exists without any chemical shift from the surface to a depth of 0.72 μm, and that the peak height of nickel decreases with depth. For silicon, two chemical forms (silicon and silicon nitride) are recognized near the surface and at depths around 0.72 μm, respectively (Fig. 7b). The peak height of silicon becomes larger closer to the surface where nickel dominates. The profile of 1s electron binding energy of nitrogen shows that titanium nitride

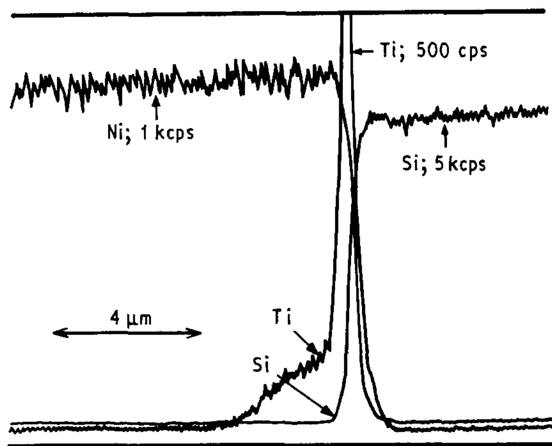

Figure 4 X-ray line analyses of silicon, nickel and titanium across the interface between silicon nitride and the adjacent nickel buffer in the specimen shown in Fig. 3b.

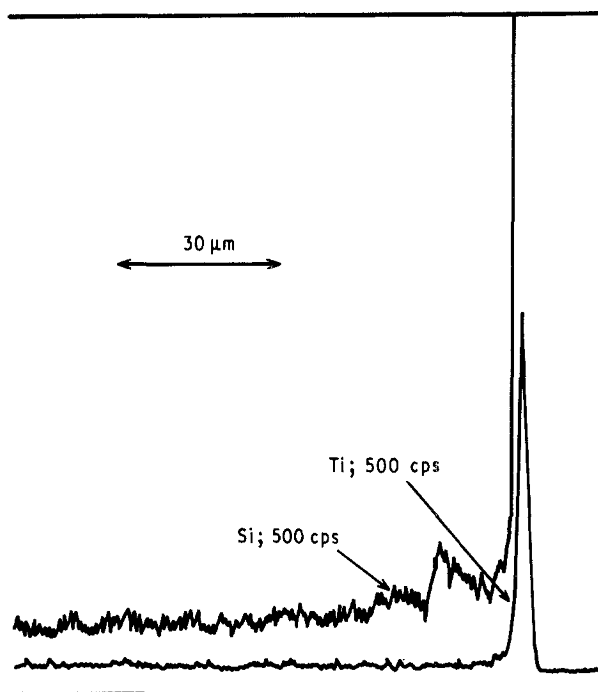

Figure 5 X-ray line analyses of silicon and titanium obtained when the detection sensitivity for silicon was raised to 10 times that used in the analyses shown in Fig. 4.

appears prominently from the sixth profile, corresponding to a depth of about 0.3–0.72 μm (Fig. 7c). These results suggest that the sputter-deposited titanium changes its chemical form into titanium nitride, and that the titanium nitride coexists with silicon nitride at depths around 0.72 μm where silicon nitride begins to dominate. Fig. 7a and b also indicates that silicon atoms diffuse into the sputter-deposited nickel film and that nickel atoms diffuse inversely to the coexisting region of silicon nitride and titanium nitride.

The other ESCA analyses were carried out using a specimen in which the sputter-deposited nickel film had been removed by chemical polishing, as Fig. 7 did not provide detailed information on interfacial reactions between the silicon nitride and sputter-deposited titanium. Fig. 8 shows the change in chemical forms of

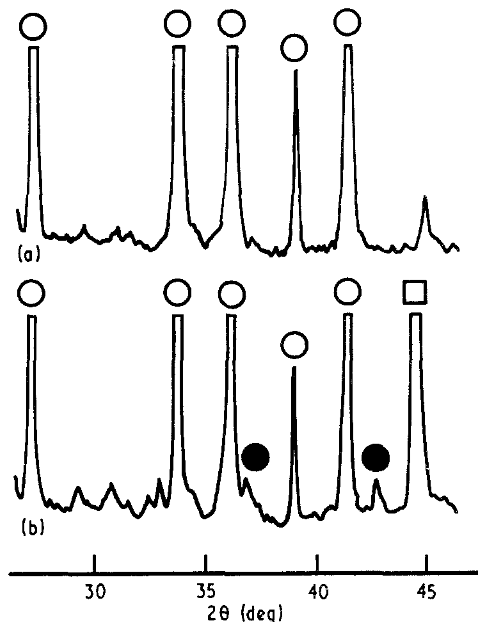

Figure 6 X-ray diffraction profiles from (a) silicon nitride; (b) silicon nitride sputter-deposited with titanium and nickel, and heated at 1423 K. ○, Si_3N_4; ●, TiN; □, Ni.

silicon and nitrogen with depth from the surface appearing after removal of the nickel film to the silicon nitride. It is obvious that only titanium nitride exists from the surface to a depth of about 0.1 μm (Fig. 8b) and that silicon nitride also appears below this depth (Fig. 8a). The formation of titanium nitride and the existence of silicon atoms in the nickel buffer and sputter-deposited nickel film, shown by EPMA and ESCA analyses, clearly indicate that a dissociation reaction of silicon nitride in contact with titanium occurs with the reaction products of titanium nitride and silicon atoms.

3.4. Mechanism of formation of the strong interface

The following formulae are obtained thermodynamically for the production of titanium nitride and titanium silicide, respectively, at 1423 K [5, 9]

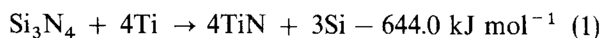

$$Si_3N_4 + 4Ti \rightarrow 4TiN + 3Si - 644.0\ \mathrm{kJ\ mol^{-1}} \quad (1)$$

and

$$Si_3N_4 + 5Ti \rightarrow Ti_5Si_3 + 2N_2 - 230\ \mathrm{kJ\ mol^{-1}} \quad (2)$$

where the free energy of formula 2 is cited from Fig. 4 of Reference 5. It is easily seen from the above formulae that titanium nitride is produced by the reaction between silicon nitride and titanium more preferentially than titanium silicide. In fact, Suganuma *et al.* [5] have shown that a very thin reaction layer, titanium nitride, is produced at the interface of the silicon nitride/2-mm-thick titanium couple, while titanium silicide several micrometres thick is produced on the side of titanium. The thickness of the sputter-deposited titanium films in the present study is smaller by four orders of magnitude than that of titanium sheet used in the study of Suganuma *et al.* [5]. Thus it is considered that titanium atoms in the sputter-deposited films are exhausted in the reaction represented by

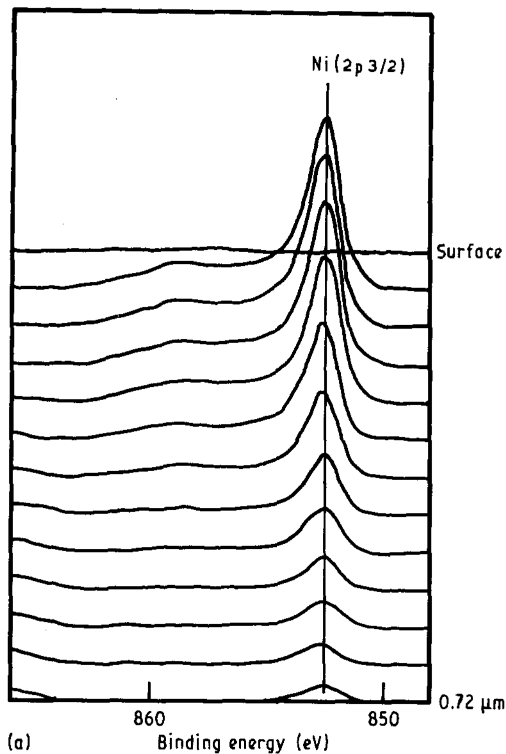

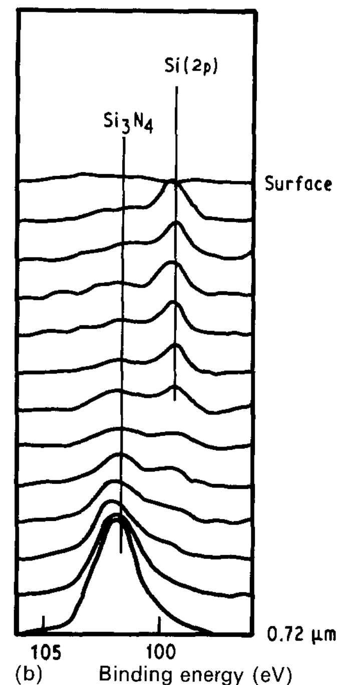

Figure 7 The shifts in binding energy of (a) nickel $2p^{3/2}$; (b) silicon 2p; (c) nitrogen 1s electrons obtained when ESCA analysis was conducted from the sputter-deposited nickel film to a depth of 0.72 μm.

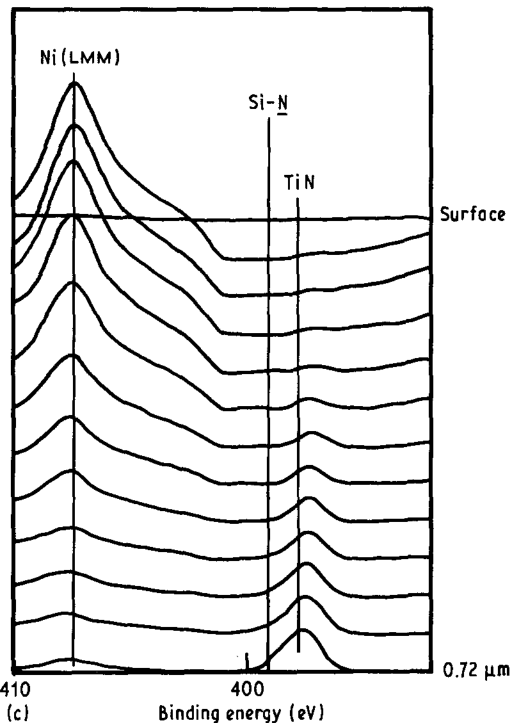

formula 1 because of these very small amounts. In addition, the very small amounts of silicon and titanium diffusing into nickel shown in Figs 4 and 5 suggest that the amounts of these elements are within the solubility limit of nickel.

As discussed above, the following interfacial reaction and diffusion across the interface are thought to take place during the joining process. Titanium in contact with silicon nitride changes its chemical form into titanium nitride. On the other hand, titanium in contact with nickel film and isolated silicon atoms (produced by the dissociation of silicon nitride) diffuse into the adjacent nickel buffer, while nickel atoms diffuse inversely into the titanium nitride. Therefore it is concluded that the strong net interfacial bond is attributed not only to such a good interface, at which the titanium nitride/silicide interface inducing a peeling off has not formed, but also to the diffusion bonding due to the interdiffusion of silicon, titanium and nickel atoms across the interface.

3.5. Reduction of thermal stress due to molybdenum buffer

It was impossible precisely to estimate thermal stress induced in the joined silicon nitride. However, when the fracture toughness of the joined silicon nitride was measured with an indentation fracture method [10, 11], the values obtained near the interface were smaller than those far from the interface. This fact indicates clearly that tensile stress remains near the interface in the joined silicon nitride. To show this, the thermal stress induced in joined silicon nitride was calculated with the two-dimensional finite-element method, and the influence of the metallic buffers on the reduction of the thermal stress was examined. Fig. 9 shows elastic displacement of silicon nitride/SUS304 stainless steel joints with and without buffer. The displacement of silicon nitride near the interface is larger in the joint without buffer (Fig. 9a) than in that with buffer (Fig. 9b). A maximum tensile stress induced in silicon nitride joined without buffer is located on the surface at a distance of 0.08 mm from the interface. However, when molybdenum and nickel buffers are inserted, the position of the maximum stress becomes about 0.4 mm distant from the silicon

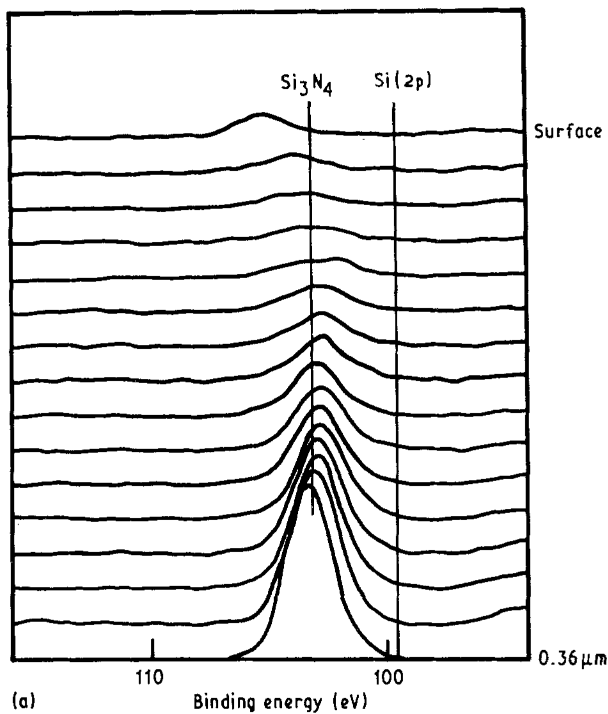

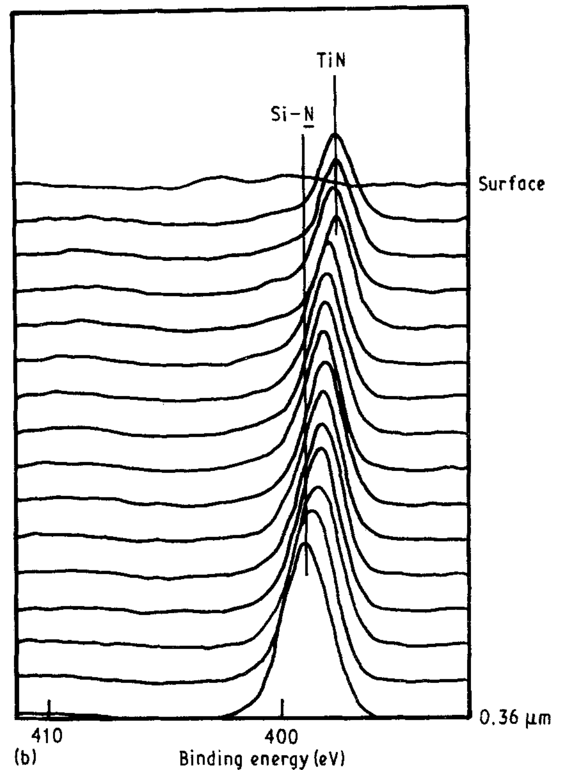

Figure 8 Shifts in binding energy of (a) silicon 2p; (b) nitrogen 1s electrons obtained when ESCA analysis was conducted from the surface which appeared after removal of the sputter-deposited nickel film by chemical polishing, to a depth of 0.36 μm.

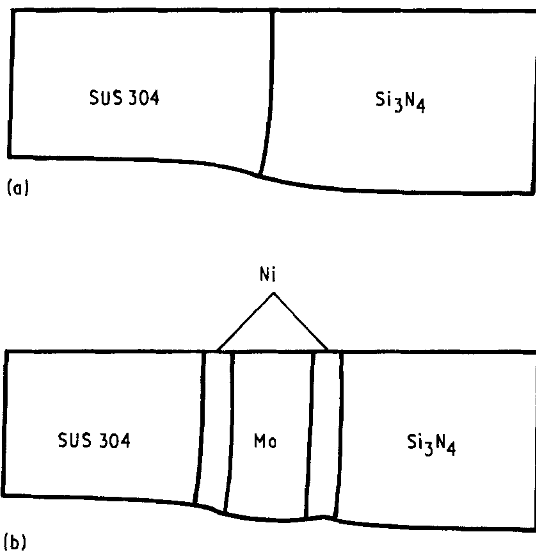

Figure 9 Elastic displacement of silicon nitride/SUS304 stainless steel joints (a) without any buffer; (b) with 1-mm-thick molybdenum and 0.5-mm-thick nickel buffers.

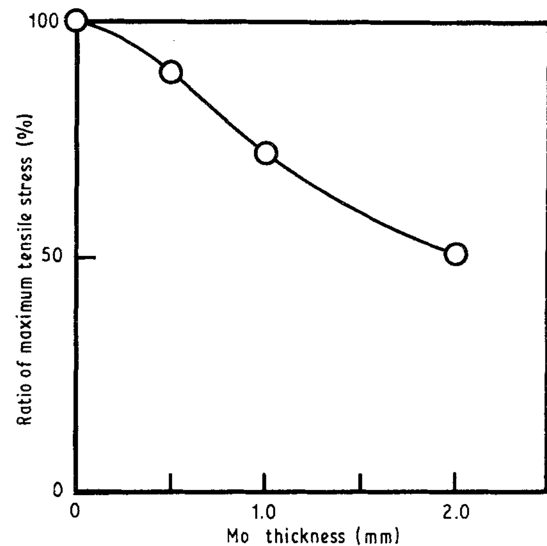

Figure 10 Change in ratio of maximum tensile stress induced in silicon nitride of the joint with a molybdenum buffer to that without buffer, as the buffer thickness is increased. Thickness of nickel buffers, 0.5 mm.

nitride/nickel buffer interface, irrespective of the thickness of molybdenum buffer.

We presented the effect of thermal stress by the ratio of the maximum tensile stress in the joint with a molybdenum buffer to that without the molybdenum buffer. Fig. 10 shows the change of the ratio with the thickness of the molybdenum buffer when the thickness of nickel buffers is constant (0.5 mm). The ratio of maximum tensile stress decreases rapidly with an increase in thickness of the molybdenum buffer. Therefore it is inferred that the insertion of the molybdenum buffer increases fracture stress of the joints, since it reduces residual tensile stress inducing the fracture at the interface between silicon nitride and the adjacent nickel buffer. When the thickness of the molybdenum buffer was constant (1 mm), the maximum tensile stress for a joint with 0.5-mm-thick nickel buffers increased only slightly (by 0.57%) compared with that for a joint without nickel buffers. It is presumed that thermal stress is unaffected by elastic deformation of nickel buffers inserted for the sputter-deposited nickel film/molybdenum and molybdenum/SUS304 joining.

4. Conclusions

Silicon nitride with thin, sputter-deposited titanium and nickel films was joined to SUS304 stainless steel using metallic buffers in a sequence of silicon nitride/nickel/molybdenum/nickel/SUS304, and the joining strength and microstructures were investigated. The fracture strength of the joints showed values up to 169 MPa with a four-point bending test. Cracks were formed at the interface between silicon nitride and the adjacent nickel buffer. They propagated along the interface or into the silicon nitride. The specimens which fractured by the propagation of cracks into the silicon nitride showed larger fracture stresses than those of the specimens in which cracks propagated along the interface. Metallographical analyses indicated that silicon nitride in contact with titanium was dissociated with reaction product of titanium nitride and isolated silicon atoms, and that titanium and silicon atoms diffused into the adjacent nickel buffer and nickel diffused inversely into the titanium nitride. Calculations using a finite-element method showed that a maximum tensile stress which arose on the surface of silicon nitride near the interface was reduced markedly with the thickness of an inserted molybdenum buffer. It is concluded from these results that the strong interfacial bond inducing the fracture of the silicon nitride is attributed to a good interfacial reaction between the silicon nitride and the sputter-deposited titanium film, the interdiffusion of silicon, titanium and nickel, and the marked reduction of thermal stress due to the insertion of the molybdenum buffer.

Acknowledgement

We wish to express our gratitude to Mr A. Kagohara (Kyocera Co.) for many useful suggestions during the course of this work.

References

1. R. L. MEHAR, and D. W. McKEE, *J. Mater. Sci.* **11** (1976) 1009.
2. M. J. BENNETT and M. R. HOULTON, *ibid.* **14** (1979) 184.
3. R. F. PABST and G. ELSSNER, *ibid.* **15** (1980) 188.
4. K. SUGANUMA, T. OKAMOTO and M. SHIMADA, *High Temp. High Press.* **16** (1985) 627.
5. K. SUGANUMA, T. OKAMOTO, Y. MIYAMOTO, M. SHIMADA and M. KOIZUMI, *Mater. Sci. Tech.* **2** (1986) 1156.
6. E. O. BALLARD, E. A. MEYER and G. M. BRENNAN, *Weld. J.* **64** (1985) 37.
7. S. MOROZUMI, M. KIKUCHI and T. NISHINO, *J. Mater. Sci.* **16** (1981) 2173.
8. M. G. NICHOLAS and R. M. CRISPIN, *ibid.* **16** (1981) 2173.
9. O. KUBASHEWSKI and C. B. ALCOCK, "Metallurgical Thermochemistry", 5th edn (Pergamon, Oxford, 1979) p. 382.
10. D. B. MARSHALL and B. R. LAWN, *J. Mater. Sci.* **14** (1979) 2001.
11. D. B. MARSHALL, B. R. LAWN and P. CHANTIKUL, *ibid.* **14** (1979) 2225.

Received 10 December 1990
and accepted 13 May 1991